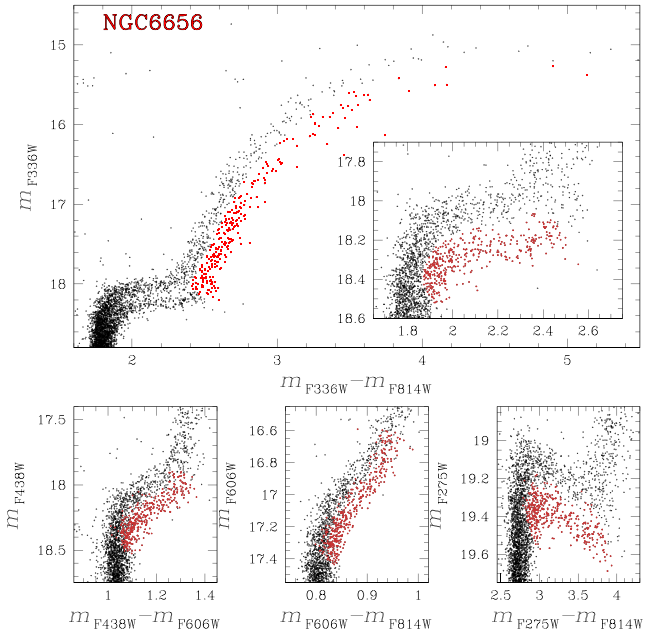

Figure 11. As in Fig. 10 but for NGC 6656.

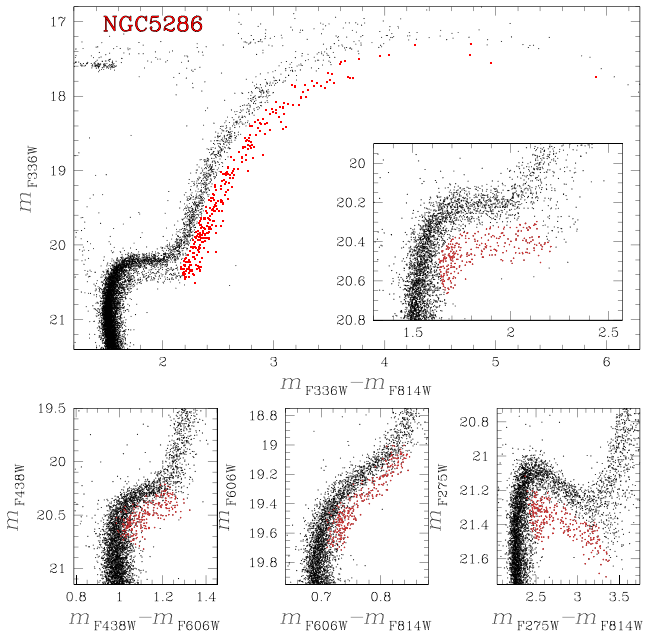

Figure 12. As in Fig. 10 but for NGC 5286.

6 UNIVARIATE RELATIONS BETWEEN MULTIPLE POPULATIONS AND GLOBAL CLUSTER PARAMETERS

In this Section, we investigate the correlation between the $W_{C\,F275W,\,F336W,\,F438W}$ and $W_{F275W,\,F814W}$ RGB widths and the 1G fraction, as determined in Section 3, and the global parameters of the host GCs. Such global GC parameters include: metallicity ([Fe/H]), absolute visual magnitude (M_V), central velocity dispersion (σ_v), ellipticity (ϵ), central concentration (c), core relaxation time (τ_c), half-mass relaxation time(τ_{hm}), central stellar density (ρ_0), central surface brightness (μ_V), reddening ($E(B-V)$), and Galactocentric distance (R_{GC}). All these quantities are taken from the 2010 edition of the Harris (1996) catalogue.

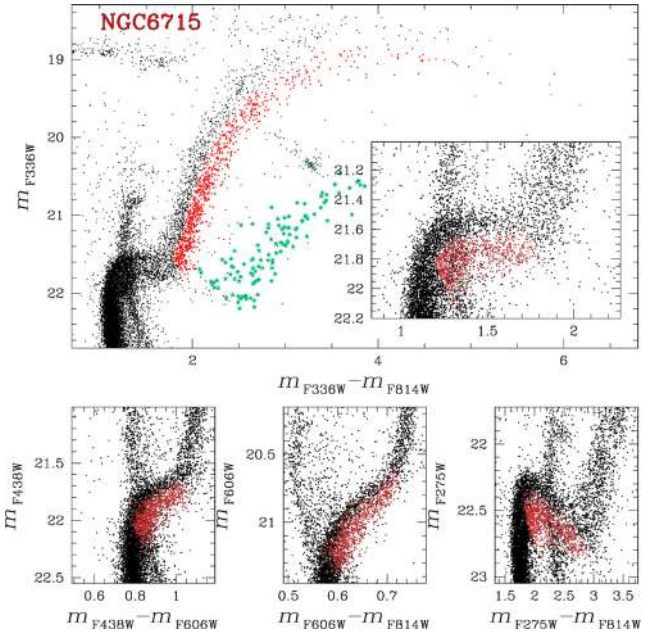

Figure 13. As in Fig. 10 but for NGC 6715. This cluster (also known as M54) sits in the core of the Sagittarius dwarf galaxy, and the CMD in the upper panel shows stars of both the cluster and the core of this galaxy. In particular, the extremely red RGB of the metal-rich population of Sagittarius' core is recognizable just to the left of the inset (aqua-starred symbols). These Sagittarius RGB stars are coloured aqua in the chromosome map of NGC 6715 shown in Fig. 5.

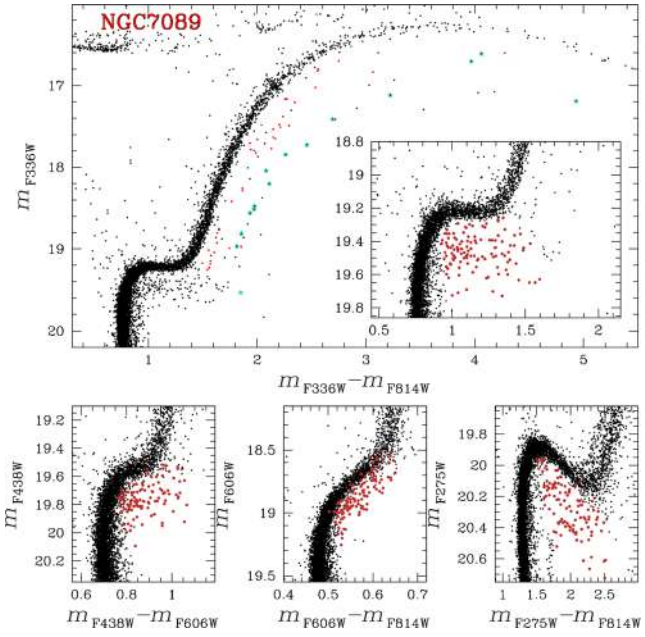

Figure 14. As in Fig. 10 but for NGC 7089. The stars in the most iron-rich RGB are represented with aqua stars.

The cluster masses have been taken from McLaughlin & van der Marel (2005) for 44 of the GCs studied in this paper. The results of our paper are based on the masses obtained by fitting the models by Wilson (1975) on the profiles of 63 Galactic GCs by Trager, King & Djorgovski (1995). The fraction of binary stars in GCs has been taken from Milone et al. (2012a), as measured within the cluster

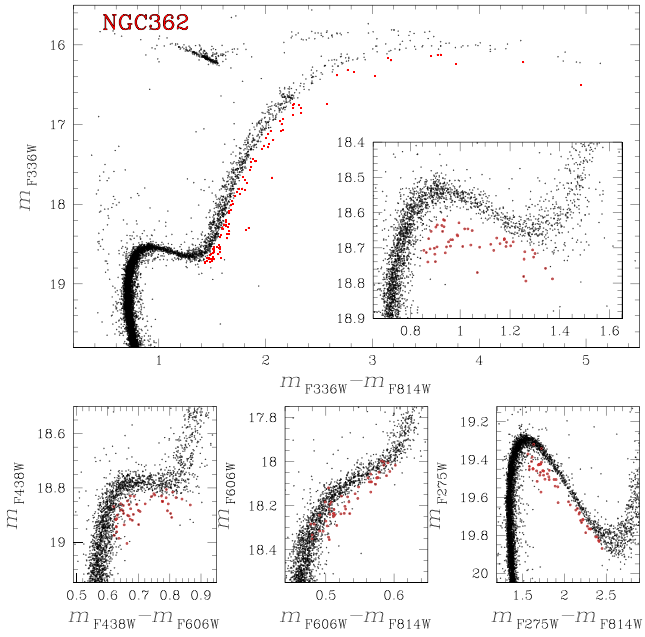

Figure 15. As in Fig. 10 but for NGC 362.

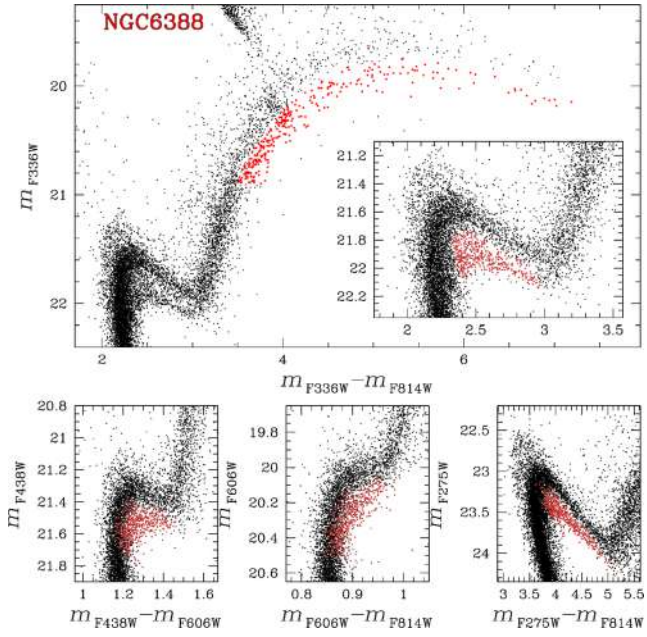

Figure 16. As in Fig. 10 but for NGC 6388.

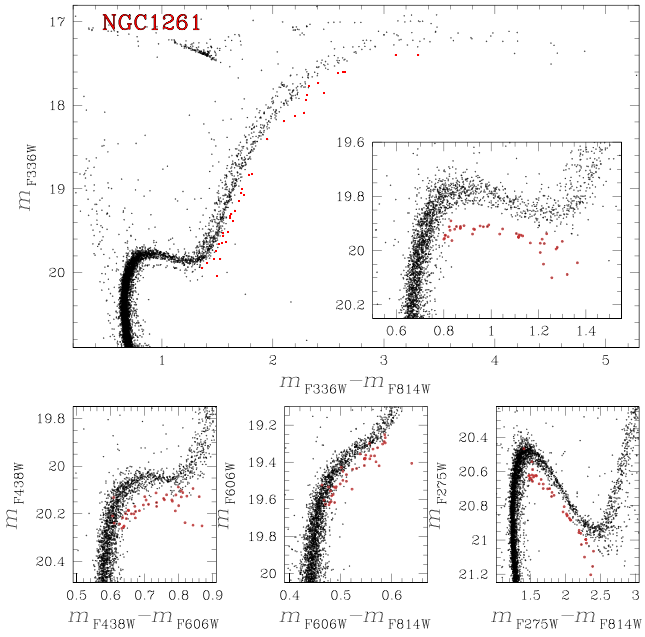

Figure 17. As in Fig. 10 but for NGC 1261.

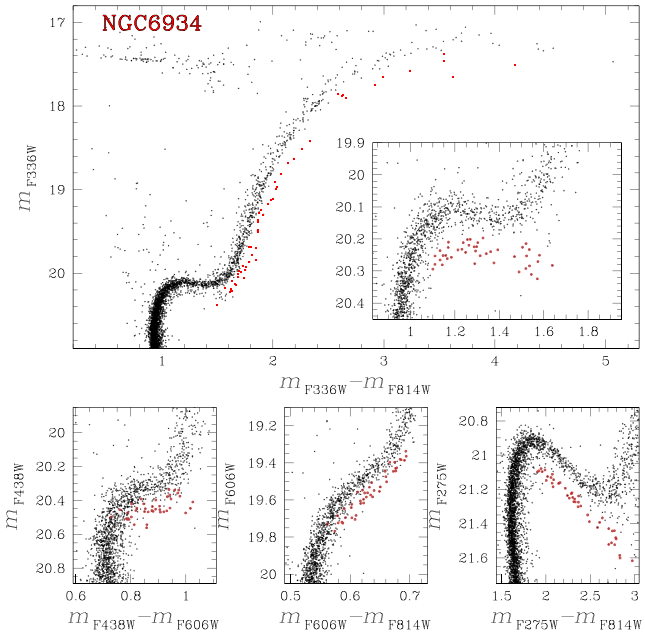

Figure 18. As in Fig. 10 but for NGC 6934.

core ($f_{\rm bin}^{\rm C}$), in the region between the core and the half-mass radius ($f_{\rm bin}^{\rm C-HM}$), and beyond the half-mass radius ($f_{\rm bin}^{\rm oHM}$).

GC ages have been taken from Marín Franch et al. (2009, hereafter MF09), Dotter et al. (2010, hereafter D10) and Vandenberg et al. (2013, hereafter V13). All ages were obtained by using the same ACS/WFC data set from Sarajedini et al. (2007) and Anderson et al. (2008) that we used in this paper, but different authors employed different sets of isochrones. The Dotter et al. (2010) sample includes 50 of the GCs studied in this paper. Additional ages for six other GCs were derived by Aaron Dotter by using the same method and are published in Milone et al. (2014).

The most recent age compilation comes from Vandenberg et al. (2013) and is based on an improved version of the classical 'vertical method', i.e. the luminosity difference between the zero-age HB and the MS turnoff. These authors have compared Victoria–Regina isochrones with GO-10775 photometry to derive the ages for 51 of the GCs that we have analysed in this paper.

When comparing two variables, we estimate the statistical correlation between the two by using the Spearman's rank correlation coefficient, r. Moreover, we associate to each value of r an uncertainty that is determined by bootstrapping statistics as in Milone et al. (2014). Briefly, we have generated 1000 equal-size resamples of the original data set by randomly sampling with replacement from the observed data set. For each i-th resample, we have determined $r_{\rm i}$ and considered the 68.27th percentile of the $r_{\rm i}$ measurements ($\sigma_{\rm r}$) as indicative of the robustness of r.